Proceedings of the ASME 2024 Heat Transfer Summer Conference
HT2024
July 15-17, 2024, Anaheim, California

SHTC2024-121705

MACHINE LEARNING ALGORITHM FOR PREDICTING HEAT TRANSFER COEFFICIENT AND PRESSURE DROP IN DIMPLED DUCTS

Mohammad Reza Shaeri[1], Andoniaina M. Randriambololona[2], Daksh Adhikari[1]
[1]Advanced Cooling Technologies, Inc., Lancaster, PA 17601, USA
[2]Department of Mechanical Engineering, University of Maryland, College Park, MD 20742, USA

ABSTRACT

Recent advances in machine learning (ML) techniques have led to a shift in strategy for predicting the hydrothermal performance of thermal management solutions. This study presents the ML-based prediction of hydrothermal performances of water-cooled dimpled ducts using an artificial neural network (ANN). The significance of the present study is to develop the ANN model using a limited number of performance data without any existing relations/correlations between input variables and outputs. Thermal and hydrodynamic performances of the ducts are represented by heat transfer coefficient and pressure drop, respectively. The input dataset for training the ANN model was prepared through a computational fluid dynamics (CFD) approach. The accuracy of the ANN model was demonstrated as such it predicted heat transfer coefficients and pressure drops of new dimpled ducts within ±17% and ±19% of true values, respectively. The present study provides a practical insight to predict the hydrothermal performance of a thermal management solution subject to limited available datapoints, and without detailed knowledge about the complex thermo-fluid physics behind the operation of the cooling system.

Keywords: Thermal management; Machine learning; Hydrothermal performance prediction; Heat transfer coefficient; Pressure drop.

1. INTRODUCTION

The accelerated miniaturization of electronic components, coupled with their increased functionality, has necessitated the development of more effective thermal management solutions to address the challenge of preventing overheating in modern electronic devices [1–5]. Dimpled surfaces have been widely identified as efficient techniques to passively improve heat transfer [6–9]. However, since dimpled surfaces are usually implemented to enhance the thermal performance of an active cooling system, the overall pumping power of the thermal management solution may substantially increase due to large pressure drops resulting from the addition of the dimples. Developing an effective active thermal management solution involves finding a balance between its thermal performance, primarily characterized by thermal resistance, and its hydrodynamic performance, represented by the pumping power [10–13]. A penalty in the pumping power may hinder using the cooling system, regardless of its capability to enhance thermal performances [14–16]. Therefore, accurately predicting both the pressure drop and thermal performance of a dimpled cooling system is essential for designing an efficient cooling system that can enhance heat transfer while operating within a practically acceptable range of pumping power. Empirical correlations developed from experimental/simulation data have been widely used to predict hydrothermal performances of cooling systems. However, conducting experiments and/or simulations to collect large numbers of data points over extensive ranges of design parameters and operating conditions requires substantial efforts and extremely high computational resources, even when utilizing current advanced computational facilities [17]. Relying on an existing bank of performance data for a cooling system from literature rather than collecting data through experiments or simulations also poses its own set of challenges. The available data may be limited in terms of the number of data points, and more significantly, these data points may be widely scattered, given that they are collected by different researchers across diverse ranges of operating and design conditions. The absence of clear relationships among these scattered data points makes the development of correlations through conventional regression and interpolation techniques extremely challenging, if not impossible [18,19].

Machine learning (ML) has been identified as a powerful technique to overcome the challenge of conducting expensive experiments and simulations for collecting data points. ML, a subset of artificial intelligence, identifies latent patterns from complex datasets and obtains the relationships between inputs and outputs with reasonable accuracy even in highly nonlinear systems [20]. This capability of ML is highly suitable to generate new outputs when there is a limited and scattered dataset available in literature for a particular application. Developing empirical correlations needs sufficient knowledge to identify key design parameters as well as their impacts on the thermo-fluid physics behind the operation of the cooling system. In the absence of such knowledge, which is very possible when the physics is complex, accuracy and efficacy of the empirical correlations remain questionable. However, ML-based models could predict the hydrothermal performance of a cooling system without any need for detailed knowledge of the complex thermo-fluid physics. A ML algorithm learns a complex pattern between inputs and outputs from the input dataset and uses this pattern to generate outputs for new inputs [21,22]. Another significance of ML is its application in optimization problems, especially when the physics behind the transport phenomena is not well understood. For an optimization process, a correlation is required to determine relationships between inputs and outputs. However, in applications with complex thermo-fluid physics, developing a physics-based model to describe such relationships is extremely challenging. However, since ML is a data-driven technique, it does not need a correlation between inputs and outputs.

In the present study, an artificial neural network (ANN) is used to predict heat transfer coefficient (h) and pressure drop (ΔP) of dimpled ducts operating in a laminar flow. The significance of the present study is that the ANN model is developed using a limited number of performance data without any existing correlations among the inputs and outputs. The ANN model identifies a pattern among four design parameters that are the input variables, and h and ΔP as two outputs. The accuracy of the model is assessed by comparing the predicted data with new performance data that have not been observed by the ANN model before. The present study provides a practical insight on the development of ML-based models for predicting hydrothermal performance of thermal management systems subjected to limited available performance datapoints.

2. COMPUTATIONAL APPROACH

2.1 Artificial Neural Network (ANN)

An artificial neural network (ANN) consists of interconnected nodes called neurons. The feed-forward multilayer ANN model, illustrated in Fig. 1, comprises of an input layer, hidden layer(s), and an output layer [23]. Input variables are received in the input layer, and outputs are generated in the output layer. Hidden layer(s) are intermediate layers used to transfer information from the input layer to the output layer. The feed-forward implies that the inputs always propagate forward through the network, which means that the outputs of all neurons in one layer act as the inputs for the neurons in the next layer [24]. Since ML is a data-driven technique, preparation of an input dataset that must consist of inputs and outputs is an essential step for the learning process of the ANN. The input dataset is randomly divided into three categories: training, validation, and testing. The input-output pattern is learned from the training dataset and the performance of the pattern is assessed by the validation dataset. When the training and validation is terminated, the accuracy of the neural network is evaluated using the testing dataset, which is a new dataset that has not been previously observed by the neural network [25].

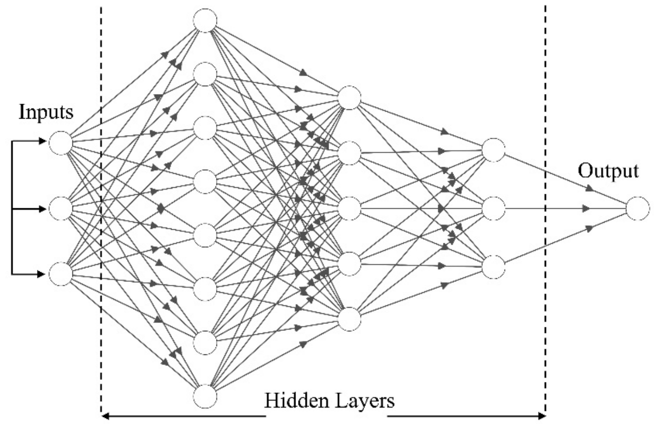

FIGURE 1: SCHEMATIC OF A MULTILAYER ANN ARCHITECTURE

Inside the neural network, each neuron is associated with weights and a bias. The output signals transferred from neurons of the (n-1)-th layer to the j-th neuron of the n-th layer is represented as follows [17,21,26]:

$$x_j^n = f_n\left(\sum_k w_{jk}^n x_k^{n-1}\right) \tag{1}$$

where w_{jk}^n corresponds to the weight from the k-th neuron of the (n-1)-th layer to the j-th neuron of the n-th layer, and f_n is the activation function of layer n. The loss function (E), which is the magnitude of the error between the predicted outputs and the true values, is calculated using an evaluation metric, which is the mean absolute error (MAE) in the present study:

$$E = \frac{1}{n}\sum_{i=1}^{n}\left|\hat{y}_i - y_i\right| \tag{2}$$

where $\hat{y}_i$ and y_i are the i-th predicted output and the true values, respectively. Then, the weights are updated using gradient descent algorithms through an iterative process, as shown below:

$$w_k = w_k - \eta\frac{\partial E}{\partial w_k} \tag{3}$$

where η is the learning rate. An optimizer is used to improve the training speed and accuracy for updating the weights. When the training process is terminated, the accuracy of the neural network is assessed by an evaluation metric, which is MAE in this study.

2.2 Problem Description

The cooling system of interest in the present study is a two-dimensional dimpled duct illustrated in Fig. 2. Since the ANN modeling strategy in the present study is not restricted to the number of dimensions, a two-dimensional duct is selected only to reduce the computational time for preparing the input dataset.

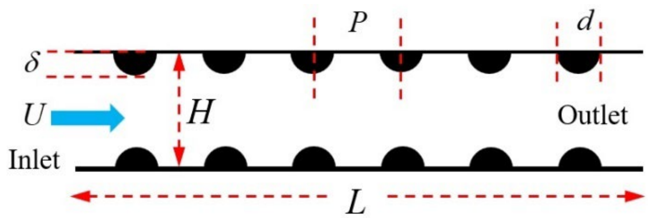

FIGURE 2: SCHEMATIC OF THE DIMPLED DUCTS IN THE PRESENT STUDY

The duct material and coolant are aluminum and water, respectively. Dimples are hemispheres that are uniformly distributed on both sides of the duct in the streamwise direction. H, L, d, P, and δ correspond to the duct height, length, dimple width, pitch (center-to-center distance), and dimple height, respectively. Due to the hemispherical geometry of the dimples, $d = 2\delta$. The relation between P and the duct length is as follows:

$$P = \frac{L}{N+1} \tag{4}$$

where N represents the number of dimples on one side of the duct. The ducts operate within laminar flow regime with a Reynold number (Re) up to 1200. The Re is defined using the half-height of the channel [27,28], as follows:

$$\mathrm{Re} = \frac{\rho U \left(H/2\right)}{\mu} \tag{5}$$

where U, ρ, and μ are the fluid velocity, density, and viscosity, respectively.

The goal of the present study is to develop an ANN-based model to predict thermal and hydraulic performance of dimpled ducts within the operating conditions and geometrical information provided in Table 1. For simplicity, it is assumed that all ducts have the same length, although the ANN model can be developed to include duct length as an additional variable. The thermal and hydraulic performance of the ducts are characterized by h and ΔP, respectively. The major significance of the present study is to develop an ANN-based model using limited available hydrothermal performance data points (137 data) within the wide geometrical and operating conditions covered in Table 1. The available data points are listed in Table 2. N_d in Table 2 represents the number of datapoints.

TABLE 1: GEOMETRICAL AND OPERATIONAL CONDITIONS OF THE DIMPLED DUCTS.

L (mm)	100
H (mm)	1 - 10
d (mm)	≥ 0.1
$N \times d/L$	≤ 0.95
Re	≤ 1200

TABLE 2: INPUT DATASET FOR TRAINING THE ANN.

H (mm)	N_d	d (mm)	N	Re
1	12	0.5	7	50, 200
		0.6	4	25, 75, 125
		0.7	9	250, 350, 450, 650
		0.8	12	200, 350, 500
2	15	0.75	19	150, 440, 640, 873
		1	15	130, 270, 363, 700
		1.2	11	263, 383, 603
		1.7	6	68, 213, 345, 370
3	13	0.8	30	170, 400, 785, 1053
		1.4	10	123, 235, 450
		1.8	21	245, 445, 780, 998
		2.3	3	100, 205
4	13	0.9	18	205, 750, 875, 1145
		1.5	28	110, 348, 558, 1130
		2	6	30, 55, 85
		3.4	9	25, 63
5	16	1	21	248, 503, 865, 1113
		2	16	163, 428, 580, 833
		2.5	8	145, 278, 483, 698
		3	4	50, 208, 465, 700
6	14	1.3	16	210, 390, 710, 1050
		2.7	11	245, 495, 673, 953
		3.6	6	118, 160, 280, 358
		5	3	45, 108
7	15	1	33	190, 568, 750, 1120
		1.7	10	218, 498, 650, 1138
		4	15	155, 410, 595, 840
		6	2	25, 50, 95
8	14	2	24	195, 345, 885, 1130
		3.4	17	133, 425, 725, 1050
		4.5	9	38, 125, 165, 248
		7.5	3	40, 50
9	13	1	26	383, 723, 1000, 1130
		4.2	7	90, 175, 238
		6.5	14	160, 293, 403
		7.6	9	70, 145, 193
10	12	3.5	20	270, 450, 900, 1135
		5.5	10	190, 495, 625
		6.5	13	190, 280, 505
		8.5	3	50, 75
Total number of data points				137

2.3 Input Data Preparation

The input dataset listed in Table 2 was prepared by simulation of steady state and two-dimensional laminar flow and heat transfer in dimpled ducts using a computational fluid dynamics (CFD) approach. The governing equations by assuming an incompressible flow and constant properties for both fluid and solid are as follows [29]:

$$\nabla . \bar{u} = 0 \tag{6}$$

$$\left(\bar{u} . \nabla\right) \rho \bar{u} = -\nabla p + \mu \nabla^2 \bar{u} \tag{7}$$

$$\bar{u} . \nabla T_f = \alpha \ \nabla^2 T_f \tag{8}$$

$$\nabla^2 T_s = 0 \tag{9}$$

where $\bar{u}$, ρ, p, μ, T_f, and α are fluid velocity, density, pressure, viscosity, temperature, and thermal diffusivity, respectively. Also, T_s is the solid temperature. The governing equations were solved using Ansys Fluent. At the inlet, fluid flow velocity and temperature of 20 °C were set. At the outlet, zero axial gradients for all the variables were imposed. The remaining surfaces were walls with a no-slip boundary condition. A constant heat flux equivalent to 200 W was applied at the bottom surface of the duct. The upper surface was adiabatic. To calculate the temperature distribution at the interface between the solid and the fluid, the conjugate problem of conduction equation with convection in the fluid were solved simultaneously [30]. The grid independence tests confirmed negligible changes in h and ΔP by increasing the number of grids beyond the selected number of computational cells for the ducts.

2.4 ANN Training

Through the training process, the ANN learns a pattern among the input variables and outputs. In this study, the input variables for training the neural network were H, d, N, and Re. The outputs were h and ΔP. The accuracy of an ANN model highly depends on selecting an appropriate network architecture and settings, which are usually determined through a trial-and-error technique. Detailed research about the dependency of the accuracy of the results to neural network architectures can be found in [19]. In this study, two multilayer feed-forward ANNs with the same architectures and settings, one of which is used for predicting h and another for predicting ΔP, were used. The only difference between the two neural networks is their output. Among 137 data points provided in Table 2, 64% and 16% were chosen randomly for training and validation, respectively. The remaining 20% was used for testing to evaluate the accuracy of the networks. The neural networks were implemented in Python. Table 3 lists detailed information on the ANN models used in this study.

TABLE 3: DETAILS OF THE ANN MODEL.

ANN type	Feed-forward multi-layer
Inputs	H, d, N, Re
Outputs	h and ΔP. Each output belongs to an individual neural network
Number of hidden layers	8
Number of neurons in hidden layers	256 neurons at each hidden layer
Loss function	MAE
Data division (training, validation, testing)	64:16:20
Batch size	24
Number of epochs	1000
Learning rate	3×10^{-4}
Activation function	ReLU
Training algorithm	Backpropagation
Optimizer	Adam

3. RESULTS AND DISCUSSION

The loss function in the present study was the MAE. Fig. 3 illustrates the MAE at different numbers of epochs (i.e., training processes) related to the training and validation of the neural network to predict h. Negligible changes in the MAE beyond 100 epochs indicates the convergence of the training process at 100 epochs.

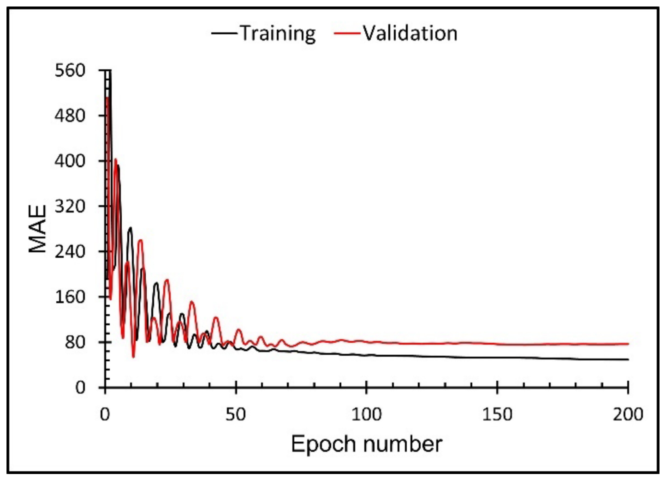

FIGURE 3: CORRESPONDING LOSS FUNCTION FOR THE TRAINING AND VALIDATION OF THE ANN TO PREDICT HEAT TRANSFER COEFFICIENT

To verify the prediction accuracy of the ANN model, the heat transfer and fluid flow for randomly selected dimpled ducts with different geometrical parameters than those provided in Table 2 but within conditions indicated in Table 1 were simulated, and their corresponding hydrothermal performances were compared with the predicted values obtained by the developed ANN model. Table 4 lists the information of the selected dimpled ducts.

Fig. 4 and Fig. 5 compare the percentage deviation from the true values for the heat transfer coefficients and pressure drops, respectively. The percentage deviation is obtained as $\left(\psi_p - \psi_t\right)/\psi_t \times 100$, where ψ indicates either h or ΔP, and the indexes p and t correspond to the predicted value by the ANN model and the true value obtained by CFD, respectively.

TABLE 4: DIMPLED DUCTS FOR EVALUATING THE PREDICTION ACCURACY OF THE ANN MODEL.

H (mm)	L (mm)	d (mm)	N	Re
2.5	100	1.2	20	300, 490, 550, 800, 1025
3.3	100	1.4	24	200, 250, 340, 525, 650, 750, 900, 1000
4.8	100	2	15	250, 375, 600, 850, 1050
5.7	100	2.8	30	300, 400, 490, 550, 650, 800, 1025
6.3	100	2.2	24	200, 340, 525, 750, 1000
8.5	100	3.2	30	490, 550, 800, 1025
Total number of data points				34

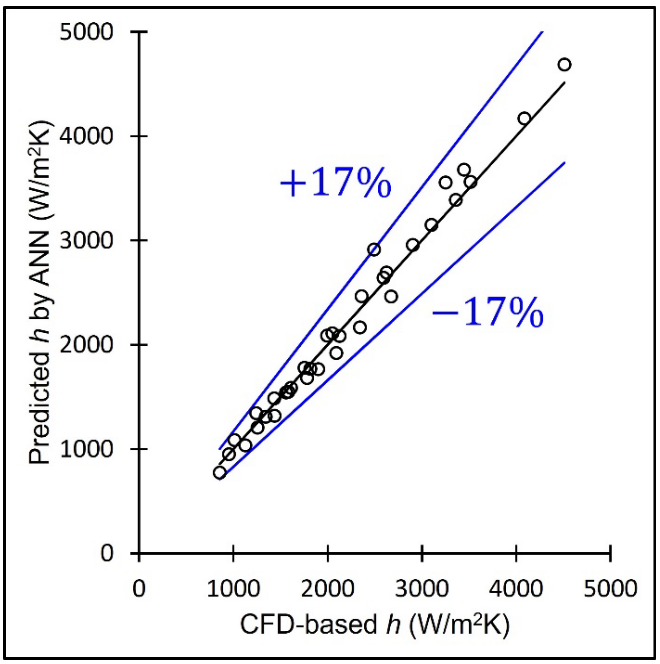

FIGURE 4: COMPARISON BETWEEN THE PREDICTED AND SIMULATED HEAT TRANSFER COEFFICIENTS FOR DIMPLED DUCTS SPECIFIED IN TABLE 4

The ANN model in the present study predicted heat transfer coefficients and pressure drops of dimpled ducts within ±17% and ±19% of true values, respectively. While these deviations may seem larger than those obtained by detailed empirical correlations, the development of such precise correlations necessitates extensive knowledge of the underlying complex physics governing the hydrothermal performance of the problem. Although training the ML algorithm with a large number of data points can result in higher prediction accuracy, the cost and time associated with computational resources and/or experimental efforts substantially increase. However, given that the neural networks in this study were trained with a limited set of data points, the good agreements between the predicted and true values suggest a satisfactory level of accuracy for the ANN model to predict the hydrothermal performance of the dimpled ducts in the present study.

The proposed modeling strategy in the present study is a general approach and is independent from the type of thermal management solution and the thermo-fluid physics behind the operation of the cooling system. However, attention should be given to preparing an appropriate input dataset that covers a sufficiently wide range of performance data. Otherwise, the ML model may underpredict or overpredict the hydrothermal performance of the cooling system.

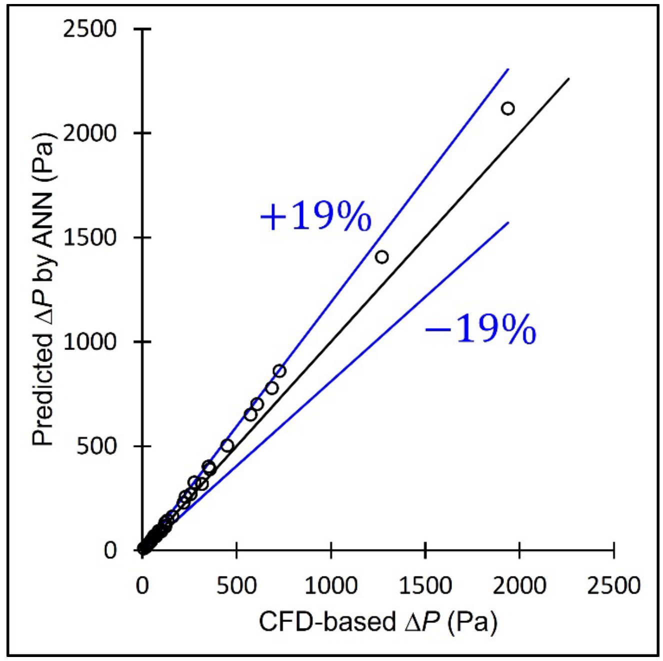

FIGURE 5: COMPARISON BETWEEN THE PREDICTED AND SIMULATED PRESSURE DROPS FOR DIMPLED DUCTS SPECIFIED IN TABLE 4

4. CONCLUSION

The capability of ANN-based models to predict the hydrothermal performances of dimpled ducts over an extensive range of design parameters and operating conditions subject to limited available performance data points was investigated. The performance of the ANN model was demonstrated by comparing the predicted and simulated performance data corresponding to six randomly selected dimpled ducts at random Re, which were not observed by the neural network before. The ANN-based model predicted heat transfer coefficients and pressure drops of new dimpled ducts within ±17% and ±19% of true values, respectively. Such good agreement, particularly when employing a limited input dataset for training the neural network, suggests that ML-based models serve as effective alternatives to expensive experimental and simulation efforts for predicting hydrothermal performances of thermal management solutions.

ACKNOWLEDGEMENTS

Support from National Science Foundation-CREST Award (Contract #HRD-1914751) and the Department of Energy/National Nuclear Security Agency (DE-FOA-0003945) provided to the University of the District of Columbia, Washington, DC is gratefully acknowledged.

REFERENCES

[1] Debich B, Yaich A, Dammak K, El Hami A, Gafsi W, Walha L and Haddar M 2021 Integration of multi-objective reliability-based design optimization into thermal energy management: Application on phase change material-based heat sinks *J. Energy Storage* **41** 102906

[2] Shaeri M R, Bonner R W and Ellis M C 2020 Thin hybrid capillary two-phase cooling system *Int. Commun. Heat Mass Transf.* **112** 104490

[3] Shaeri M R, Bonner R and Catuche J 2023 Additively Manufactured Hybrid Two-Phase Cold Plate *ASME 2023 International Technical Conference and Exhibition on Packaging and Integration of Electronic and Photonic Microsystems* ASME 2023 International Technical Conference and Exhibition on Packaging and Integration of Electronic and Photonic Microsystems (San Diego, California, USA: American Society of Mechanical Engineers) p V001T07A001

[4] Shaeri M R, Chen C-H, Bonner R W and Demydovych M 2023 Demonstration of CTE-Matched Two-Phase Minichannel Heat Sink *2023 22nd IEEE Intersociety Conference on Thermal and Thermomechanical Phenomena in Electronic Systems (ITherm)* (Orlando, FL, USA: IEEE) pp 1–5

[5] Catuche J, Shaeri M R and Ellis M C 2022 Additive Manufacturing of Capillary-Driven Two-Phase Cold Plates *Proceedings of the 8th World Congress on Mechanical, Chemical, and Material Engineering (MCM'22)* (Czech Republic, Prague) p HTFF 174

[6] Piper M, Zibart A, Djakow E, Springer R, Homberg W and Kenig E Y 2019 Heat transfer enhancement in pillow-plate heat exchangers with dimpled surfaces: A numerical study *Appl. Therm. Eng.* **153** 142–6

[7] Rao Y, Zhang P, Xu Y and Ke H 2020 Experimental study and numerical analysis of heat transfer enhancement and turbulent flow over shallowly dimpled channel surfaces *Int. J. Heat Mass Transf.* **160** 120195

[8] Chen Y, Liu Z and He D 2020 Numerical study on enhanced heat transfer and flow characteristics of supercritical methane in a square mini-channel with dimple array *Int. J. Heat Mass Transf.* **158** 119729

[9] Li M, Chen X and Ruan X 2020 Investigation of flow structure and heat transfer enhancement in rectangular channels with dimples and protrusions using large eddy simulation *Int. J. Therm. Sci.* **149** 106207

[10] Shaeri M R and Bonner R W 2018 Lightweight and high-performance air-cooled heat sinks *2018 34th Thermal Measurement, Modeling & Management Symposium (SEMI-THERM)* 2018 34th Thermal Measurement, Modeling & Management Symposium (SEMI-THERM) (San Jose, CA: IEEE) pp 224–7

[11] Shaeri M R 2018 THE KEY ROLE OF PUMPING POWER IN ACTIVE COOLING SYSTEMS *Proceeding of 3rd Thermal and Fluids Engineering Conference (TFEC)* 3rd Thermal and Fluids Engineering Conference (TFEC) (Fort Lauderdale, USA: Begellhouse) pp 1181–4

[12] Randriambololona A M and Shaeri M R 2022 Thermal Performances of Multi-Layered Liquid Cold Plates The 8th World Congress on Mechanical, Chemical, and Material Engineering

[13] Shaeri M R and Bonner R 2019 ADVANCES IN LIGHTWEIGHT HEAT SINKS *Proceeding of 4th Thermal and Fluids Engineering Conference* 4th Thermal and Fluids Engineering Conference (Las Vegas, NV, USA: Begellhouse) pp 839–42

[14] Shaeri M R, Bonner R and Pearlman H 2017 ENHANCING HEAT TRANSFER RATES ACROSS DIFFERENT FLOW REGIMES USING PERFORATED-FINNED HEAT SINKS *Proceeding of Second Thermal and Fluids Engineering Conference* Second Thermal and Fluids Engineering Conference (Las Vegas, USA: Begellhouse) pp 843–52

[15] Botchway K-D and Shaeri M R 2022 The Effect of Locations of Inlet and Outlet Manifolds on Thermal Performance of a Lithium-Ion Battery Thermal Management System The 7th World Congress on Momentum, Heat and Mass Transfer

[16] Randriambololona A M and Shaeri M R 2022 Hydrothermal Performances of Liquid Cold Plates The 7th World Congress on Momentum, Heat and Mass Transfer

[17] Qiu Y, Garg D, Zhou L, Kharangate C R, Kim S-M and Mudawar I 2020 An artificial neural network model to predict mini/micro-channels saturated flow boiling heat transfer coefficient based on universal consolidated data *Int. J. Heat Mass Transf.* **149** 119211

[18] Chen Z and Cao F 2016 Scattered data approximation by neural networks operators *Neurocomputing* **190** 237–42

[19] Shaeri M R, Randriambololona A M and Sarabi S 2022 Prediction Accuracy of Artificial Neural Networks in Thermal Management Applications Subject to Neural Network Architectures *Proceedings of the 8th World Congress on Mechanical, Chemical, and Material Engineering (MCM'22)* (Prague, Czech Republic)

[20] Ding R, Zhang S, Chen Y, Rui Z, Hua K, Wu Y, Li X, Duan X, Wang X, Li J and Liu J 2022 Application of Machine Learning in Optimizing Proton Exchange Membrane Fuel Cells: A Review *Energy AI* **9** 100170

[21] Shaeri M R, Sarabi S, Randriambololona A M and Shadlo A 2022 Machine learning-based optimization of air-cooled heat sinks *Therm. Sci. Eng. Prog.* **34** 101398

[22] Randriambololona A M, Shaeri M R and Sarabi S 2022 Artificial Neural Network Models to Predict Heat Transfer Coefficients and Pressure Drops in Cold Plates with Surface Roughness *Proceedings of the 8th World Congress on Mechanical, Chemical, and Material Engineering (MCM'22)* (Prague, Czech Republic)

[23] Salgado C M, Dam R S F, Puertas E J A and Salgado W L 2022 Calculation of volume fractions regardless scale deposition in the oil industry pipelines using feed-forward multilayer perceptron artificial neural network and MCNP6 code *Appl. Radiat. Isot.* **185** 110215

[24] Santosh K, Das N and Ghosh S 2022 Deep learning: a review *Deep Learning Models for Medical Imaging* (Elsevier) pp 29–63

[25] Cheng X, Ren F, Gao Z, Zhu L and Huang Z 2022 Synergistic effect analysis on sooting tendency based on soot-specialized artificial neural network algorithm with experimental and numerical validation *Fuel* **315** 122538

[26] Moon J, Gbadago D Q, Hwang G, Lee D and Hwang S 2022 Software platform for high-fidelity-data-based artificial neural network modeling and process optimization in chemical engineering *Comput. Chem. Eng.* **158** 107637

[27] Sano M and Tamai K 2016 A universal transition to turbulence in channel flow *Nat. Phys.* **12** 249–53

[28] Nakabayashi K and Kitoh O 1996 Low Reynolds number fully developed two-dimensional turbulent channel flow with system rotation *J. Fluid Mech.* **315** 1–29

[29] Botchway K-D and Shaeri M R 2022 The Effect of Outlet Manifold Location of Liquid-Cooled Battery Thermal Management Systems on Pumping Power The 8th World Congress on Mechanical, Chemical, and Material Engineering

[30] Botchway K-D and Shaeri M R 2022 Hydrothermal Performance of Liquid-Cooled Battery Thermal Management System with Multiple Inlets 9th International Conference on Fluid Flow, Heat and Mass Transfer (FFHMT'22)